Ankle-Angle Estimation from Blind Source Separated Afferent Activity in the Sciatic Nerve for Closed-Loop Functional Neuromuscular Stimulation System

Kang-Il Song, Jun-Uk Chu, *Member, IEEE*, Sunghee E. Park, Dosik Hwang, and Inchan Youn*

***Abstract*—Cuff electrode recording has been proposed as a solution to obtain robust feedback signals for closed-loop controlled functional neuromuscular stimulation (FNS) systems. However, single-channel cuff electrode recording requires several electrodes to obtain the feedback signal related to each muscle. In this study, we propose an ankle-angle estimation method in which recording is conducted from the proximal nerve trunk with a multichannel cuff electrode to minimize cuff electrode usage. In experiments, muscle afferent signals were recorded from a rabbit's proximal sciatic nerve trunk using a multichannel cuff electrode, and blind source separation and ankle-angle estimation were performed using fast independent component analysis (PP/FastICA) combined with dynamically driven recurrent neural network (DDRNN). The experimental results indicate that the proposed method has high ankle-angle estimation accuracy for both situations when the ankle motion is generated by position servo system or neuromuscular stimulation. Furthermore, the results confirm that the proposed method is applicable to closed-loop FNS systems to control limb motion.**

***Index Terms*—Ankle-angle estimation, artificial neural network, blind source separation, functional neuromuscular stimulation (FNS) system, multichannel cuff electrode, muscle afferent neural signal.**

Manuscript received February 22, 2016; revised May 16, 2016; accepted June 7, 2016. Date of publication June 14, 2016; date of current version March 17, 2017. This work was supported in part by a grant from the Korea Health Technology R&D Project through the Korea Health Industry Development Institute, funded by the Ministry of Health & Welfare of the Republic of Korea under Grant HI14C3477, and the Next-generation Medical Device Development Program for Newly-Created Market of the National Research Foundation, funded by the Korean government, MSIP (No 2015M3D5A1066100). *Asterisk indicates corresponding author.*

K.-I. Song is with the Biomedical Research Institute, Korea Institute of Science and Technology, and also with the School of Electrical and Electronic Engineering, Yonsei University.

J.-U. Chu is with the Daegu Research Center for Medical Devices and Rehabilitation Engineering, Korea Institute of Machinery and Materials.

S. E. Park is with the Biomedical Research Institute, Korea Institute of Science and Technology and also with the School of Mechanical Engineering, Korea University.

D. Hwang is with the School of Electrical and Electronic Engineering, Yonsei University.

*I. Youn is with the Biomedical Research Institute, Korea Institute of Science and Technology, Seoul 02792, South Korea, and also with the Korea University of Science and Technology, Seoul 02792, South Korea (e-mail: iyoun@kist.re.kr).

Digital Object Identifier 10.1109/TBME.2016.2580705

I. Introduction

FUNCTIONAL neuromuscular stimulation (FNS) is a promising method for rehabilitating weakened or lost muscle function in disabled people [1]. When applied to an intact peripheral nerve or muscle, functional movements can be restored in patients with stroke, spinal cord, or peripheral nerve injuries. Most FNS systems used in the clinical field consist of preprogrammed stimulation parameters that facilitate the modulation of a desired movement by changing the stimulation intensity. These conventional approaches require continuous or repeated stimulation that leads to premature muscle fatigue and tissue damage [2]. In recent studies [3]–[5], closed-loop FNS systems were proposed using an artificial sensor or a natural sensor as a feedback signal. In terms of closed-loop control, robust feedback signals are needed to ensure correct timing when applying the stimulation. Artificial sensors, such as goniometers and foot switches, have been widely used in closed-loop FNS systems. However, these artificial sensors have limitations caused by cosmetic problems and have recalibration requirements due to environmental interference. As an alternative to using artificial sensors, natural sensors have been used to provide useful information on specific targeted sensory or motor organs. For example, the cutaneous afferent activities generated by exteroceptive sensors in the skin have been used to control grasping [6] and to correct a foot drop [7], whereas the muscle afferent activities generated by proprioceptive sensors in the muscle spindle have been used to control the ankle angle [8].

Cuff electrode recording is known to be an effective approach for extracting information and realizing feedback control in FNS systems [9]–[11]. In the case of ankle-angle control for patients with motor function disorders, several approaches have been proposed using the sensory information extracted from cuff electrode recordings. Jensen *et al.* [3] demonstrated a closed-loop FNS system that uses the muscle afferent as a feedback signal. To estimate the ankle angle, the muscle afferents are recorded from the tibial and peroneal nerves, and electrical pulses are delivered to the tibialis anterior and lateral gastrocnemius muscles to generate the flexion and extension of the ankle joint. Strange *et al.* [4], [5] demonstrated a closed-loop FNS system for gait assistance. In their research, the muscle afferents are recorded from the distal median or distal radial nerves, to which electrical pulses are applied to sequentially stimulate each related muscle. Cavallaro *et al.* [12] demonstrated the feasibility of a

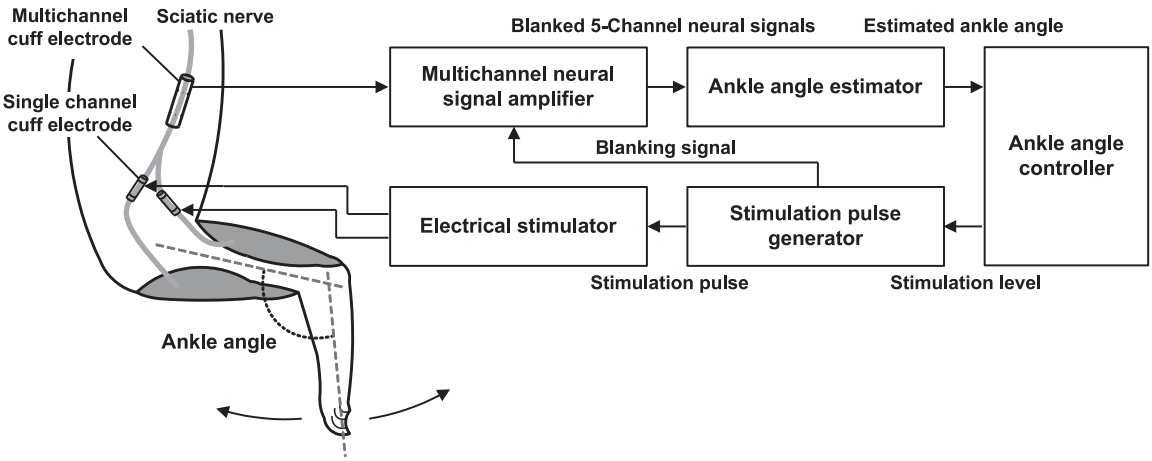

Fig. 1. Block diagram of the closed-loop FNS system using multichannel cuff for ankle-angle control.

closed-loop system for standing motion using the muscle afferents recorded from the tibial and peroneal nerves. However, in most previous studies, the cuff electrodes were implanted on the distal branches of a multifascicular nerve to measure the afferent signals from the targeted muscles. In addition, several cuff electrodes were simultaneously implanted onto the nerve branches within a narrow space. This often resulted in a spatial limitation because the nerve branches to the innervated muscles are usually too short and thin to place the nerve cuff electrode at the implantation site.

With regard to the feasibility of implantation, it is more desirable that the recording site of cuff electrodes be closer to the proximal root of a multifascicular nerve than the distal branches. Typically, a proximal nerve trunk consists of multiple fascicles; for example, the sciatic nerve trunk includes the tibial and peroneal nerves, which are separated above the knee and innervate the dorsiflexor muscles and the plantar-flexor muscles, respectively. Multichannel cuff electrodes have been proposed to achieve selective recording of the neural activity of a multifascicular nerve [13], [14]. These multichannel cuff electrodes provide the aggregate neural activities of the multiple fascicles. In previous studies, various source separation methods have been attempted to recover the neural activity of the individual fascicles. Wodlinger *et al.* [15] identified each fascicle in simulated multichannel neural signals using a beamforming algorithm. They modeled the multichannel neural signals as a linear combination of the neural activities of multiple fascicles, which were shown to be suitable for source localization and for the recovery of the neural activity of the individual fascicles. Other related methods have also been suggested using blind source separation and linear regression. For example, Tesfayesus *et al.* [16] performed a simulation experiment to recover each fascicular neural signal from a multichannel cuff electrode. They represented the multichannel neural signals using a finite element model based on a linear combination of the individual fascicular signals, which were recovered by the blind source separation method. Their results showed that blind source separation was suitable for decomposing the multifascicular nerve signal. Cheng *et al.* [17] performed an *in vivo* experiment to record the muscle afferent signals using a multichannel cuff electrode. They were able to decompose the neural signals detected from the sciatic nerve into the tibial and peroneal components using a linear regression model. However, the linear regression model should have the original source signals recorded from the tibial and peroneal nerves to model the multichannel sciatic nerve signals. Furthermore, the two channel sciatic nerve signals needed to be manually selected to maximize the separability. When a closed-loop FNS system using multichannel cuff electrodes is applied in clinical trials, a source separation method should be learned in an unsupervised manner and conducted without any intervention by the user. These techniques have exhibited some level of separability for mixed multifascicular nerve signals obtained from multichannel electrodes. However, the present series of studies focused on the decomposition of the nerve signals. To construct a closed-loop FNS system for ankle-angle control, a robust feedback signal should be provided in a form such as a continuous stream of estimated ankle angles.

To address these considerations, this paper presents an ankle-angle estimation method using multichannel signals recorded from the sciatic nerve trunk. Our approach combines a blind source separator and an ankle-angle estimator. For source separation, we used an unsupervised linear projection that exhibited greater separability performance. Moreover, a dynamic neural network exhibited greater estimation accuracy than an ankle-angle estimator. On the sciatic nerve trunk, a multichannel cuff electrode recording was performed to estimate the ankle angle without additional recordings from the peroneal and tibial nerves, which is advantageous as fewer nerve cuff electrodes are used. Specifically, we used a projection pursuit method based on fast independent component analysis (PP/FastICA), which was more capable of extracting discriminative signals from the sciatic nerve. These separated neural signals were used to estimate the ankle angle by applying a dynamically driven recurrent neural network (DDRNN). This combination of the two methods exhibited high ankle-angle estimation accuracy for both situations when the ankle motion was generated by a position servo system and neuromuscular stimulation.

The proposed ankle-angle estimation method using multichannel neural signals is a part of the overall FNS system for feedback control of ankle angle by neural signal recordings and electrical stimulation (see Fig. 1). To achieve ankle-angle control, the ankle angle is estimated from the muscle afferent signals and sent to the ankle-angle controller as a feedback signal. The stimulation level is then adjusted to minimize the error between the desired and estimated angles. In this scheme, obtaining robust feedback signals is important factor to

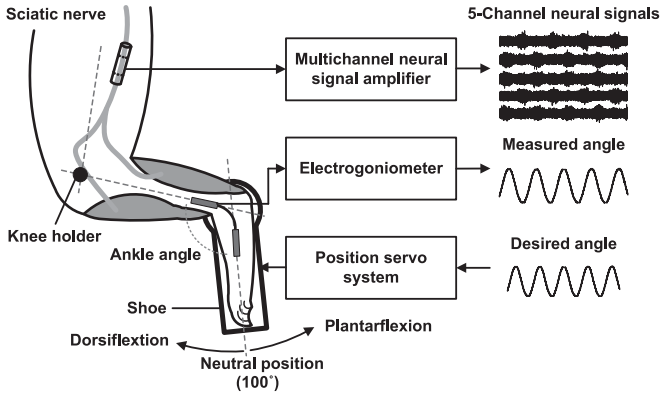

Fig. 2. Experimental setup for multichannel recordings during passive movements.

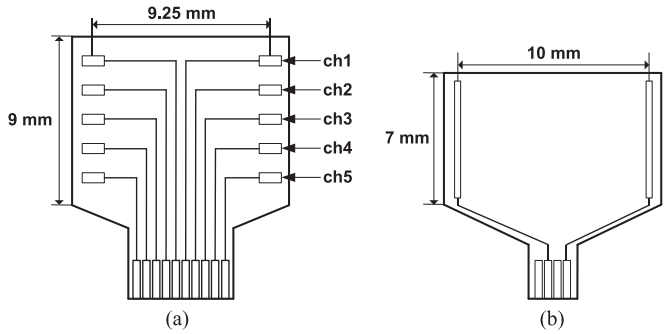

Fig. 3. Picture of (a) five-channel cuff and (b) single-channel cuff.

facilitate closed-loop control. Here, we show that the proposed multichannel neural recordings and motion estimation method could be a possible approach to obtain robust feedback signals for closed-loop controlled FNS system.

II. Methods

A. Data Acquisition

Animal experiments in which neural signals from the sciatic nerve were recorded during passive ankle movements were carried out. Five adult male New Zealand white rabbits weighing 2–2.5 kg were used in the experiments. The rabbits were kept and handled in accordance with the regulations of the Institutional Animal Care and Use Committee of the Korea Institute of Science and Technology. The overall animal experimental scheme is shown in Fig. 2. The multichannel cuff was constructed on a polyimide substrate with platinum electrodes. The polyimide substrate was self-biased to curl into a roll with an inner diameter. As shown in Fig. 3(a), the five-channel cuff had ten platinum electrodes, and the pair of electrodes on both sides was connected to the neural signal recording system in a bipolar configuration. Each electrode was 1-mm-wide and 0.5-mm-long. The diameter of the cuff was 1.8 mm, and the distance between electrodes was 9.25 mm. The nerve cuff was positioned 1 cm above the point at which the sciatic nerve is divided into two branches as the tibial and peroneal nerves.

For neural signal recording, the cuff electrode system developed in a previous study [18] was modified to accommodate the multichannel cuff electrode. An implantable amplifier module and an external amplifier module with a gain of 39601 and a –3-dB bandwidth from 425 to 5500 Hz were connected during neural signal recording. The implantable amplifier module was located in a subcutaneous pocket on the hip of each New Zealand white rabbit, and a transcutaneous connector was mounted over the iliac crest. The angular position of the ankle joint was measured using an electrogoniometer (SG 65, Biometrics) positioned on the side of the tibia and the foot. The five-channel sciatic nerve signals, which were the final output of the external amplifier, and the angular position were simultaneously digitized using an analog-to-digital converter board (PXI-6733, National Instruments) with a 16-bit resolution and a sampling frequency of 25 kHz. In addition, a single-channel cuff (see Fig. 3(b)) was also implanted on the tibial and peroneal nerves, respectively. The tibial and peroneal nerve signals were simultaneously recorded during passive ankle movements using the same cuff electrode system. These neural signals were used to evaluate the source separation performance for the multichannel signals recorded from the sciatic nerve trunk.

B. Passive Ankle Flexion–Extension Trial

Ankle motion was generated by a computer-controlled position servo system. A servomotor (HS-7954SH, Hitec) was used to elicit ankle movement, and a shoe was fastened to the foot. The motor shaft was aligned with the ankle axis of the foot shoe. This system enabled the ankle to be rotated at programmable rates through a sinusoidal trajectory in the sagittal plane. The ankle angle was defined as the inside angle between the tibia and the foot using the coordinate system shown in Fig. 2. The neutral position was defined as 100°, and full flexion (dorsiflexion) and full extension (plantarflexion) were defined as 70° and 130°, respectively. This passive ankle flexion–extension trial was modified from that used by Riso *et al.* [19]. To investigate the performance of the proposed method for various ankle-angle frequencies, the ankle angle was varied through a sinusoidal trajectory at different frequencies (0.3 and 0.5 Hz). In the experiments, data were collected from five normal rabbits during passive flexion–extension trials. For each rabbit, ten sessions were conducted at each frequency, and each session continued for 20 s. The overall system was controlled using LABVIEW (National Instrument, USA).

C. Ankle-Angle Estimation With Blind Source Separation

In this section, we outline the combined blind source separation and ankle-angle estimation scheme used to construct a feedback signal for the closed-loop system. The multichannel sciatic nerve signals were separated into the tibial and peroneal components using a PP/FastICA. The superpositioned nerve signal was assumed to be a linear combination of different fascicle signals because the proximal nerve trunk consists of multiple fascicles. Typically, these fascicle signals are difficult to measure due to the spatial limitation at the implantation site. Therefore, the PP/FastICA was evaluated for its potential as an unsupervised linear decomposing algorithm. Then, the ankle angle was estimated from the separated nerve signals using a DDRNN. The neuromuscular system is known to be a nonlinear dynamic system [20]. According to the characteristics of the

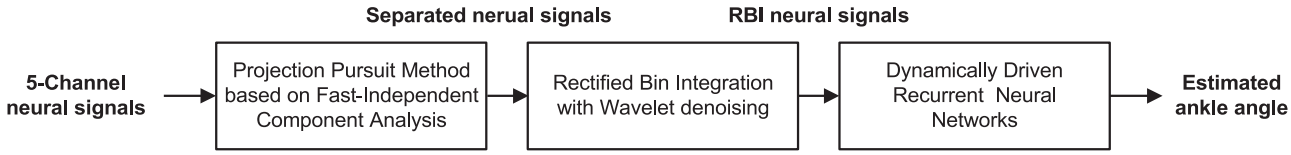

Fig. 4. Block diagram of the proposed ankle-angle estimation method for the multichannel cuff recordings.

neuromuscular system, we investigated the use of dynamic neural networks for ankle-angle estimation from the muscle afferent signals. Fig. 4 shows a block diagram of the proposed ankle-angle estimation method for multichannel cuff electrode recordings. In the following sections, we describe each block in detail.

1) Blind Source Separation: Projection Pursuit Based on Fast Independent Component Analysis: Blind source separation was performed using a PP/FastICA. The PP method is a linear transformation that preserves the underlying shape of the distribution at a high dimensionality and can determine a projection that maximizes the degree of the mutual independence in the estimated source signals [21]–[23]. Considering the experimental setup, the sciatic nerve has independent neural sources inside the nerve trunk, such as the tibial, peroneal, and sural fascicles. These neural signals project to the superficial region of the sciatic nerve trunk. Therefore, the recorded multichannel signal from each electrode can be modeled as a linear mixture of the projected signals from all sources as follows:

$$\mathbf{x} = \mathbf{A}\mathbf{s} \tag{1}$$

where $\mathbf{x}$ is the n-dimensional observed signals from the multichannel cuff electrode, $\mathbf{s}$ is m-dimensional source signals, and $\mathbf{A}$ is an $m \times n$ unknown mixing matrix. If an $m \times n$ demixing matrix $\mathbf{W}$ can be found to maximize the mutual independence of the estimated source signals, the estimated source signals $\mathbf{s}$ can be obtained from

$$\mathbf{s} = \mathbf{W}\mathbf{x}. \tag{2}$$

In this study, we used the fact that an objective function that measures the negative entropy (negentropy) of a variable is equivalent to one that measures the mutual independence of source signal using the PP method. As the PP method was implemented with FastICA, the problems related to the processing time could be solved. Practically, to estimate the source signals $\mathbf{s}$, an objective function that approximates the negentropy $J(\mathbf{s})$ was developed as a fast and robust algorithm for independent component analysis, and is referred to as FastICA [24]. $J(\mathbf{s})$ is defined as $J(\mathbf{s}) = H(\mathbf{s}_G) - H(\mathbf{s})$, where $H(\mathbf{s})$ is the entropy of $\mathbf{s}$ [21], such that it directly signifies the measure of non-Gaussianity, and it is set to zero for a Gaussian random vector. Here, $\mathbf{s}_G$ is a Gaussian random vector with the same mean and variance as $\mathbf{s}$. To compute the value of $\mathbf{W}$ that maximizes $J(\mathbf{s})$, we utilized a batch-type learning algorithm. The overall procedure of the PP/FastICA is as follows:

1) Collect the data in a matrix $\mathbf{X} = [\mathbf{x}_1\ \mathbf{x}_2\ \ldots\ \mathbf{x}_N]$.
2) Center the data by $\mathbf{X} = \mathbf{X} - E\{\mathbf{X}\}$, and whiten the data by $\mathbf{Z} = \mathbf{M}\mathbf{X}$, where $\mathbf{M} = \mathbf{E}\mathbf{V}^{-0.5}\mathbf{E}^{\mathbf{T}}$ is the whitening matrix, $\mathbf{E}$ is the matrix of the eigenvectors, and $\mathbf{V}$ is the diagonal matrix of the eigenvalues.
3) Set the number of projection pursuit directions to m, and select a random initial transformation matrix $\mathbf{W}$ of size $n \times m$.
4) Calculate the optimum projection direction using $\mathbf{W} = E(\mathbf{Z}G'(\mathbf{W}^{\mathbf{T}}\mathbf{Z})) - E(G''(\mathbf{W}^{\mathbf{T}}\mathbf{Z}))\mathbf{W}$, where G is assumed to be $-\exp(-\mathbf{U}^2/2)$, and $\mathbf{U}$ is given by $\mathbf{U} = \mathbf{W}^{\mathbf{T}}\mathbf{Z}$.
5) Orthogonalize $\mathbf{W}$ by $\mathbf{W} = \mathbf{W}(\mathbf{W}^{\mathbf{T}}\mathbf{W})^{-0.5}$.
6) Measure the similarity between the previous $\mathbf{W}$ matrix and the current$\mathbf{W}$ matrix.
7) If no convergence has occurred, go to step 4.
8) If convergence has occurred, form the projection matrix $\mathbf{W}$ of size $m \times n$ by $\mathbf{W} = \mathbf{W}^{\mathbf{T}}\mathbf{M}$.
9) Compute $\mathbf{s}_i = \mathbf{W}\mathbf{x}_i$, $i = 1, 2, \ldots, N$ as a lower-dimensional representation of the observed neural signal.

2) Angle Estimation: Dynamic Driven Recurrent Neural Network: The ankle angle was estimated using a DDRNN. Before performing the ankle-angle estimation, preprocessing was conducted. The preprocessing output was the rectified bin integration (RBI) of the separated nerve signal. The RBI of the neural signal is easy to implement and proper for high signal-to-noise ratio (SNR) applications [25]. The preprocessing sequence was as follows: First, wavelet denoising was performed to detect the action potentials buried in the noise and to improve the SNR. Wavelet denoising is a technique that can be used to reduce the background noise that can be approximated as a Gaussian distributed random source [26], [27]. In this study, a five-level time-invariant wavelet decomposition scheme using the Symmlet 7 mother wavelet was adopted because of its similarity to the typical action potential of waveforms. Hard thresholding was used with level-dependent thresholds equal to three times the standard deviation of the corresponding wavelet coefficients at each level of decomposition. Second, RBI was performed. The data windows were defined as having a 20-ms period. Finally, after this series of preprocesses was complete, two separated nerve signals—the tibial and peroneal components—were used as the inputs of the angle estimator.

In this study, to model the dynamics of the neuromuscular system, the DDRNN was constructed as follows:

$$\mathbf{y}(n+1) = \mathbf{F}(\mathbf{y}(n), \ldots, \mathbf{y}(n-p+1), \mathbf{s}(n), \ldots, \mathbf{s}(n-q+1))$$

where $\mathbf{F}$ is a nonlinear mapping, and the present value of the output $\mathbf{y}(n+1)$ is defined in terms of its past values $\mathbf{y}(n), \ldots, \mathbf{y}(n-p+1)$ and the present and past values of the input $\mathbf{s}(n), \ldots, \mathbf{s}(n-q+1)$. The DDRNN ankle-angle estimator consisted of three layers. The input layer was set by 20 neurons corresponding to the tibial and peroneal components with an input delay of 200 ms ($p = 10$). The hidden layer was set at 50 neurons. The output layer was selected by one neuron unit to estimate the ankle angle. The output signal was feedback to the input layer with an output delay of 200 ms ($q = 10$). This

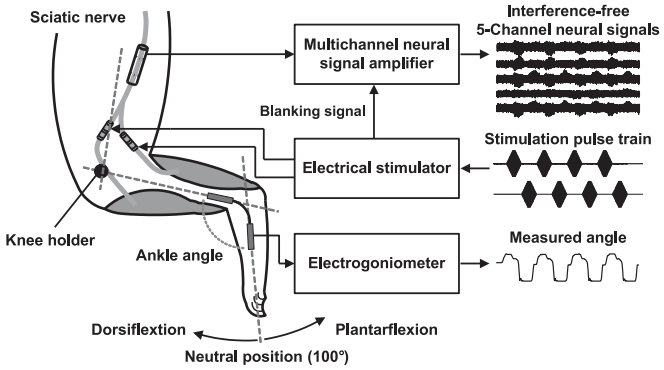

Fig. 5. Experimental setup for multichannel recordings during neuromuscular stimulation.

feedback loop represented the dynamics between the separated nerve signals and the ankle angle. In the learning procedure, the number of iterations for back-propagation learning was determined by trial and error to minimize the learning error.

D. Performance Evaluation

To evaluate its performance for source separation from the multichannel recorded signals, the PP/FastICA was compared with two other unsupervised dimension reduction methods: factor analysis (FA) and principal component analysis (PCA). Specifically, the source separation results obtained by each method were compared with the tibial and peroneal nerve signals recorded using the two single-channel cuffs (see Section II-A). Next, to verify the ankle-angle estimation performance from the separated nerve signals, the DDRNN was compared with the radial basis network (RBN) and the time-delayed neural network (TDNN) during various ankle movements (see Section II-B).

Both the separation accuracy and the estimation accuracy were evaluated from the correlation coefficients (CCs). For the source separation accuracy, the CCs were performed to determine the similarities between the original nerve signals from each single-channel cuff and the separated nerve signals from the multichannel cuff. In addition, for the ankle-angle estimation accuracy, the measured ankle angle and the estimated ankle angle were compared for similarity. The CCs were calculated using

$$R = \frac{\mathrm{cov}(x, y)}{\sqrt{\mathrm{cov}(x)\mathrm{cov}(y)}} \tag{3}$$

where in calculating the source separation accuracy, x signified the preprocessed nerve signals from each single-channel cuff, and y signified the separated nerve signals from the multichannel cuff. Conversely, in calculating the ankle-angle estimation accuracy, x signified the ankle angle measured from the electrogoniometer, and y signified the estimated ankle angle based on the separated nerve signals.

The statistics were based on the dataset from the five rabbits. For each rabbit, the performance of the proposed method was evaluated using 20-fold cross validation. Among 20 sessions for two different frequencies, one session was randomly selected as the test set, whereas the remaining sessions were used as the training set. This was repeated such that each session was used once as the test set. A one-way analysis of variance was used to remove the effect of different rabbits. Values with $p < 0.05$ were considered to be significantly different.

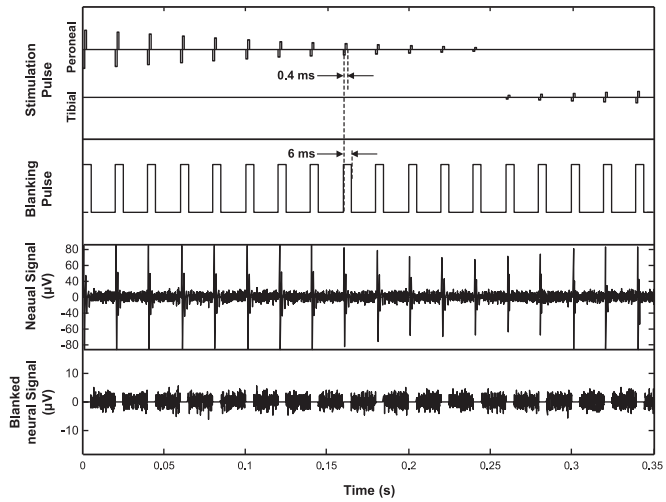

Fig. 6. Interference-free recording scheme with blanking processes.

E. Ankle-Angle Estimation During Neuromuscular Stimulation

To examine the feasibility of the proposed method in estimating ankle angle under neuromuscular stimulation, ankle motion was generated by electrical stimulation through the single-channel cuff electrode implanted on each tibial and peroneal nerve. An electrical stimulator (AM 2200, AM-system) with programmed pulse generator was used to provide a biphasic current pulse train (see Fig. 5). The rest of the experimental setup was the same as in the passive ankle flexion–extension trial (see Section II-B). In FNS applications, the interference of the stimulus artifacts and evoked electromyogram signals appear in the recordings of the neural signals [4]. To eliminate this interference, a blanking process synchronized to the stimulation was applied. During electrical stimulation, the stimulation repetition frequency was set to 50 Hz and the pulse width was 0.4 ms. The amplitude of the stimulation pulse was modulated within a range of 100 μA to be a trapezoidal shape (rising time: 0.5 s, holding time: 0.2 s, and falling time: 0.5 s). The neuromuscular stimulation was provided to each tibial and peroneal nerve over 20 s. Meanwhile, a synchronized blanking pulse with each stimulus switched the neural signal to ground for a duration of 6 ms. As a result, 14 ms of interference-free multichannel neural signals was obtained (see Fig. 6). The same blind source separation and ankle-angle estimation schemes were used as described in Section II-C. Ankle-angle estimation was performed using the proposed combination of PP/FastICA and DDRNN from the interference-free multichannel neural signals.

III. Results

A. Nerve Signal Recording From the Sciatic Nerve Trunk With a Multichannel Cuff

Fig. 7 shows the multichannel cuff recording from the sciatic nerve trunk and the single-channel cuff recording from the tibial

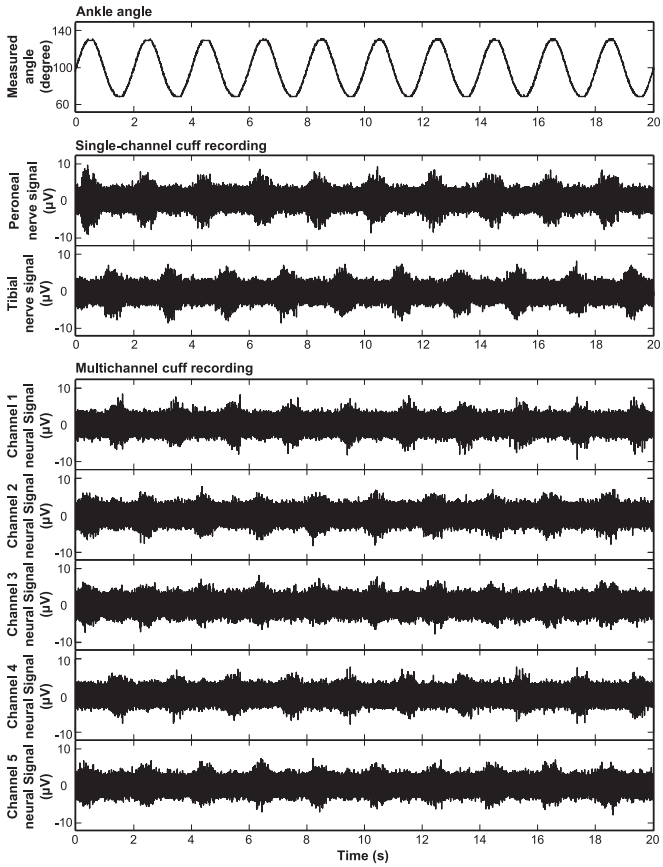

Fig. 7. Single-channel and multichannel neural signals during passive movements.

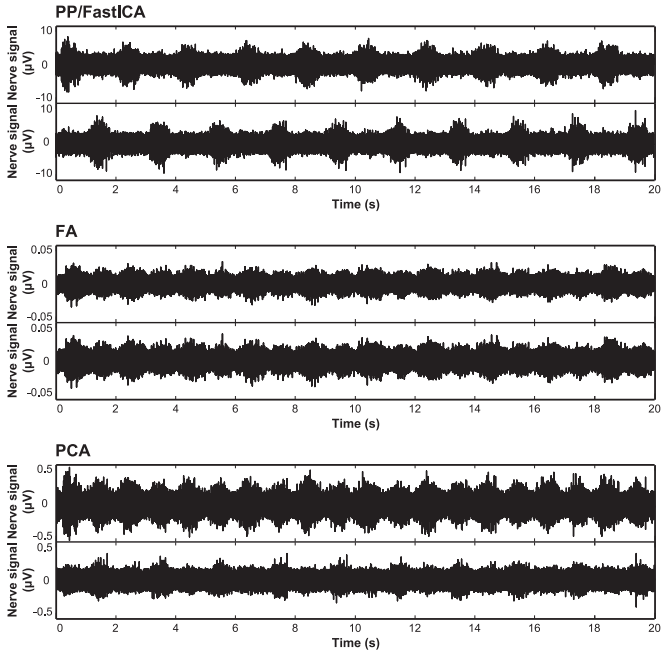

Fig. 8. Blind source separation results from the multichannel cuff recordings using the following three methods: PP/FastICA, FA, and PCA.

and peroneal nerves during a passive sinusoidal movement. This plot shows a typical example for rabbit A. The ankle-angle plot shows the angular trajectory of the ankle during passive movement, which was a flexion–extension trial within 60° and with a frequency of 0.5 Hz in a sinusoidal trajectory. The single-channel cuff recording plot shows the neural signal recorded from the tibial and peroneal nerves. The tibial and peroneal nerve signals showed an approximate 90° phase delay during the sinusoidal change in the ankle angle. The multichannel cuff recording plot shows the superposition of the tibial and peroneal nerve signals.

B. Comparison of Different Blind Source Separation and Ankle-Angle Estimation Methods

1) Blind Source Separation Method: Table I lists the source separation accuracy for the different separation methods. The PP/FastICA was found to be superior to the PCA method by an average of 0.47 ($p < 0.05$) at the tibial nerve and 0.46 ($p < 0.05$) at the peroneal nerve and superior to the FA method by an average of 0.35 ($p < 0.05$) at the tibial nerve and 0.35 ($p < 0.05$) at the peroneal nerve. Fig. 8 shows that the PP/FastICA method exhibited the greatest separation result compared with the FA and PCA methods. Table II summarizes the source separation accuracy for the different source separation methods at different frequencies. The results obtained using the PP/FastICA showed consistent source separation accuracy for both frequencies.

2) Ankle-Angle Estimation Method: Table III lists the ankle estimation accuracy for the different estimation methods using the different separation methods. The combination of PP/FastICA and DDRNN achieved the greatest $R^2 = 0.995$ among all the combinations of methods. Table IV describes the ankle-angle estimation accuracy for the different estimation methods at different frequencies. The results with DDRNN showed consistent ankle-angle estimation accuracy for both frequencies.

C. Ankle-Angle Estimation During Passive Movement

Fig. 9 shows a representative example of source separation from the recorded multichannel cuff signals using the PP/FastICA and ankle estimation using the DDRNN. The source separated neural signal plots show the recovered tibial and peroneal components from the multichannel recordings, where the overlapped gray traces denote the RBI values. The R^2 between the original neural signals and the separated neural signals were 0.826 and 0.783 for the tibial and peroneal nerves, repectively. The ankle-angle estimation plot shows the results for the ankle-angle estimation. The solid line is the measured ankle-angle trajectory, whereas the dashed line is the estimated ankle angle. The R^2 value between the original signal and the estimated signal was 0.995.

D. Ankle-Angle Estimation During Neuromuscular Stimulation

Fig. 10 shows a multichannel recording obtained from the sciatic nerve trunk during neuromuscular stimulation. By inducing the trapezoidal electrical stimulation train on each tibial and peroneal nerve, the ankle angle was generated within a range of

TABLE I
SOURCE SEPARATION ACCURACY FOR DIFFERENT SEPARATION METHODS

	PP/FastICA		FA		PCA	
Rabbit	Tibial	Peroneal	Tibial	Peroneal	Tibial	Peroneal
A	0.826	0.832	0.455	0.442	0.322	0.316
B	0.891	0.871	0.499	0.474	0.426	0.395
C	0.883	0.88	0.485	0.482	0.384	0.377
D	0.835	0.857	0.472	0.491	0.312	0.324
E	0.815	0.839	0.442	0.455	0.342	0.357
Mean	0.85	0.85	0.47	0.46	0.35	0.35
± SD	± 0.03	± 0.02	± 0.02	± 0.02	± 0.04	± 0.03

TABLE II
SOURCE SEPARATION ACCURACY FOR DIFFERENT SEPARATION METHODS AT DIFFERENT FREQUENCIES

	PP/FastICA		FA		PCA	
Frequency	Tibial	Peroneal	Tibial	Peroneal	Tibial	Peroneal
0.3 Hz	0.812	0.805	0.432	0.441	0.312	0.315
0.5 Hz	0.826	0.824	0.451	0.453	0.322	0.327
Mean	0.82	0.81	0.44	0.45	0.32	0.32
± SD	± 0.01	± 0.01	± 0.01	± 0.01	± 0.01	± 0.01

TABLE III
ANKLE-ANGLE ESTIMATION ACCURACY FOR DIFFERENT ESTIMATION METHODS WITH DIFFERENT SEPARATION METHODS

Separation Method \ Estimation Method	DDRNN	TDNN	RBN
PP/FastICA	0.995	0.892	0.881
FA	0.776	0.683	0.679
PCA	0.798	0.769	0.726

TABLE IV
ANKLE-ANGLE ESTIMATION ACCURACY FOR DIFFERENT ESTIMATION METHODS AT DIFFERENT FREQUENCIES

Frequency	DDRNN	TDNN	RBN
0.3 Hz	0.932	0.880	0.872
0.5 Hz	0.995	0.892	0.881
Mean ± SD	0.96 ± 0.01	0.89 ± 0.01	0.88 ± 0.01

60°. The angular trajectory exhibited an unsymmetrical shape due to the nonlinear characteristics of the neuromuscular system [28]. The stimulus artifacts and evoked electromyogram signals were eliminated based on the interference-free scheme; it can be confirmed in the multichannel cuff recording plot. Similar to the multichannel neural signals during passive movements, the neuromuscular stimulation generated the muscle afferent signals of the tibial and peroneal nerves, which were superposed on the multichannel neural signals.

Fig. 11 shows the results of source separation from the interference-free multichannel neural signals using PP/FastICA and ankle estimation using DDRNN. The source separated neural signals show the separated tibial and peroneal components

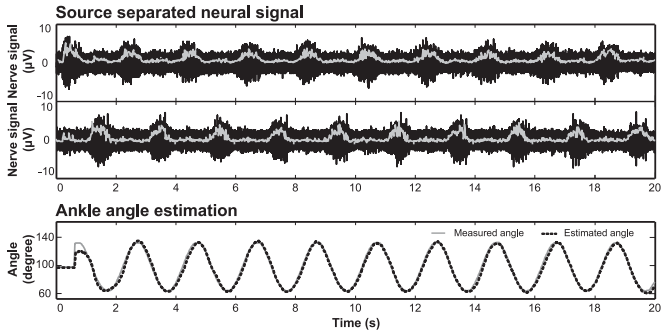

Fig. 9. Source separation and ankle-angle estimation result from multichannel neural signals during passive movements.

from interference-free multichannel neural recordings, where the overlapped gray traces denote the RBI values. In ankle-angle estimation plot, the solid line is the measured ankle angle, whereas the dashed line is the estimated ankle angle (R^2 = 0.981).

IV. DISCUSSION

In this study, an ankle-angle estimation method was developed to predict the ankle angle under multichannel cuff recording from a proximal nerve trunk. In previous studies, muscle afferent signals from the tibial and peroneal nerves were used as feedback signals for ankle-angle control [3], [9]–[11]. These approaches showed that the muscle afferent signal with a single-channel cuff is an effective feedback signal for a closed-loop FNS system. However, to obtain the muscle afferent signal using a single-channel cuff, the electrode was positioned on the distal nerve branches of each muscle, resulting in spatial limitation. Conversely, our recording approach could overcome this spatial limitation by placing the multichannel cuff on the proximal nerve trunk.

A series of independent component analyses requires two assumptions: statistical independence and linear mixing. The individual fascicular signals were found to have statistical independence, and the multichannel signals obtained at the contacts of the multichannel cuff were a linear mixture of the fascicular source signals [29]. Therefore, multichannel cuff recordings from the proximal nerve trunk could satisfy assumptions for the application of independent component analyses to recover the individual fascicular signals.

The proposed ankle-angle estimation method from the proximal nerve trunk recordings comprised of two steps: blind source separation followed by ankle-angle estimation. For blind source separation, the PP/FastICA method was proposed because it exhibited better source separation performance than other unsupervised separation methods, such as FA and PCA. FA and PCA are well-known unsupervised learning-based dimensionality reduction methods. These methods assume that the source data are normalized to zero mean and possess a Gaussian distribution. Furthermore, only covariance between the observed variables is used in the estimation. FA tries to describe the covariance relationships among variables in terms of a few unobservable random quantities called factors. The factors are assumed to be uncorrelated, which also implies independence

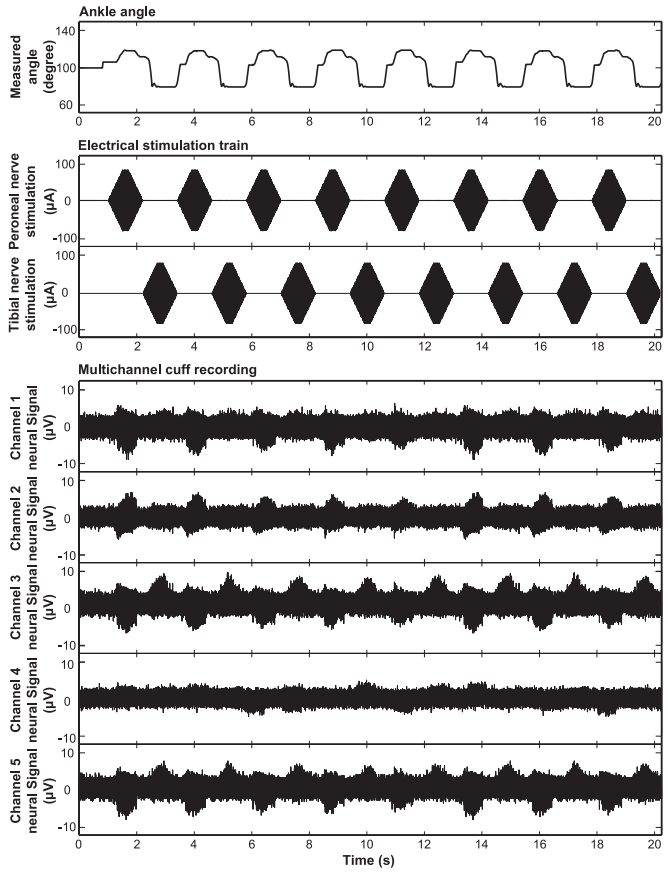

Fig. 10. Interference-free multichannel neural signals during neuromuscular stimulation.

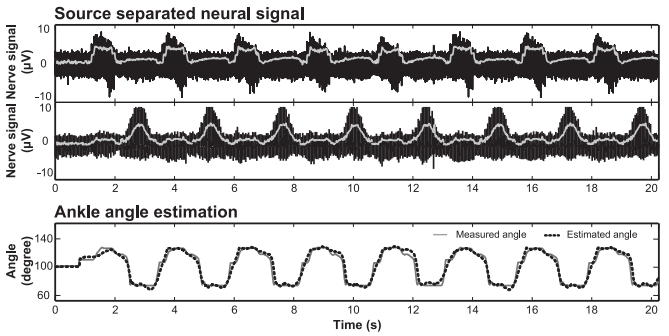

Fig. 11. Source separation and ankle-angle estimation results from interference-free multichannel neural signals during neuromuscular stimulation.

in the case of Gaussian data. PCA determines the maximum variance direction along the orthogonal direction. PCA is conducted using the eigenvalue of a data covariance matrix. With Gaussian data, determining the independent components is a simple process because uncorrelated components are always independent. Although, FA and PCA are known to be similar statistical methods, the FA considers common variance in the data, whereas PCA results in PCs that consider the maximal amount of variance of observed variables [30]. PP/FastICA is a projection that maximizes the degree of mutual independence in the estimated source signals. In this case, the PP method seeks the latent non-Gaussian structure within the observations and has an advantage that the characteristics of the high-dimensional original data are preserved [23]. Therefore, FA and PCA are adequate only when the source data have Gaussian distributions. Conversely, PP seeks one projection at a time such that the extracted signal is as non-Gaussian as possible. Consequently, FA and PCA were used to find the independent components based on the Gaussian data and could not separate the tibial and peroneal components. In contrast, PP/FastICA successfully separated the tibial and peroneal components (see Fig. 8). Therefore, we justify our choice of PP/FastICA for unsupervised source separation. In addition to the investigation of source separation accuracy, different frequencies were considered in this study. The muscle afferent signal was evoked by a muscle stretch motion that was influenced by the speed and position variations [31]. The muscle afferent signal was influenced by different frequencies, and the amplitude of the muscle afferent signals at 0.3 Hz was greater than that at 0.5 Hz. As shown in Table II, all separation methods were related to the various frequencies. However, PP/FastICA appears to have greater source separation accuracy.

Next, for ankle-angle estimation using the separated neural signals during passive movement, the proposed DDRNN exhibited a significant estimation accuracy improvement compared with other estimation methods: RBN and TDNN. RBN and TDNN are parts of an artificial neural network. In the case of RBN, to estimate the ankle-angle within predetermined error bounds, it was assumed that the radial basis function was used as the activation function and that the network structure was a feed-forward type. In this study, RBN assumed a nonlinear approximation to estimate the ankle-angle. In the case of TDNN, a feed-forward type was assumed to estimate the ankle-angle with input delay. This architecture has been shown to effectively learn the temporal dynamics of signals. In the literature, the neuromuscular system has inherent complexities, such as nonlinear, time-varying, time-delay, and redundant properties [32]. To estimate the ankle-angle, several researchers have investigated dynamic neural network methods, which exhibit compensated nonlinear and dynamic properties. In this study, the DDRNN method was used to design an output feedback node that compensated for the nonlinear dynamic properties. These properties improved the ankle-angle estimation performance compared with other estimation methods such as RBN and TDNN. In addition, the investigations of the ankle-angle estimation accuracy for different separation methods and frequencies showed that the source separation accuracy is a major factor that determines the result of the ankle-angle estimation accuracy (see Tables III and IV). Although the different frequencies influenced the ankle-angle estimation accuracy, the combination of PP/FastICA and DDRNN exhibited greater estimation accuracy than other estimation methods.

To examine the feasibility of ankle-angle estimation for FNS application, the proposed method was applied to interference-free multichannel neural signals during neuromuscular stimulation. As with the ankle-angle estimation results during passive ankle movements, the ankle-angle estimation from interference-free multichannel neural signals exhibited high ankle-angle estimation accuracy. However, base-line drift was

observed in the neural signal recordings during electrical stimulation. Although blanking processes were executed to eliminate the interference noise, such as electrical stimulation artifact and evoked electromyogram signals, the base-line drift caused by the offset voltage in the stimulation cuff electrode affected the multichannel neural signals. Therefore, the tibial and peroneal components were less separated from the interference-free multichannel neural signals than during passive movements. By rejecting the offset voltage using a charge-balanced electrical stimulation, the estimation performance could be improved.

For real-time implementation, all processes should be completed within the interval between the stimulation pulses. The concept underlying the real-time closed-loop FNS system using the proposed method is that the recorded multichannel neural signals within the electrical stimulation period are processed to decide the following electrical stimulation used to control the ankle angle. Throughout the experiments, the proposed method required a processing time of 63 μs (PP/FastICA: 10 μs and DDRNN: 53 μs, average of ten trials) to estimate the ankle angle from multichannel neural signals (MATLAB on a 2.4 GHz Core i5 PC). Considering the electrical stimulation period (20 ms) and the processing time for ankle-angle estimation ($<$1 ms), the proposed estimation method is applicable to real-time FNS systems for neural signal-based closed-loop control.

The feasibility of blind source separation for neural signals has been investigated in several studies [13], [14], [16], [17]. In these studies, excellent performance was exhibited in separating the compounded nerve signals. Nevertheless, the studies were primarily focused on decomposition of multifascicular neural signals. For ankle-angle estimation from muscle afferent signals, neural networks have been known to be an effective approach to predict ankle angle [33], [34]. Although these studies exhibited high performance, the neural signals were obtained from the distal branches of the nerve using single-channel cuffs. This experimental scheme has limitation that the single-channel cuffs are implanted onto the nerve branches within a narrow space to obtain information on specific targeted muscles. In this study, we showed that the combination of PP/FastICA and DDRNN can estimate the ankle angle from a multichannel cuff electrode positioned on the sciatic nerve trunk. By recording the multichannel neural signal from the nerve trunk, the spatial limitation resulting from being positioned on the distal branches of the nerve was overcome. Furthermore, we demonstrated that the ankle angle can also be estimated during neuromuscular stimulation. This proximal nerve trunk recording approach using a multichannel cuff and the proposed ankle-angle estimation method shows promise as an alternative method to obtain feedback signals in closed-loop FNS systems.

V. Conclusion

This paper proposed an ankle-angle estimation method that uses a multichannel cuff electrode for ankle-angle control in closed-loop FNS systems, with the sciatic nerve trunk selected as the place to conduct neural signal recordings to minimize surgical complications. The combination of PP/FastICA and DDRNN showed that it is possible to integrate a feedback signal processing method into a closed-loop FNS system. First, in the blind source separation stage, the multichannel sciatic nerve signals were separated into tibial and peroneal components using the PP/FastICA. PP/FastICA is based on a fixed-point iteration scheme that maximizes non-Gaussianity as a measure of statistical independence. In addition, PP/FastICA learned in an unsupervised manner because a source separation method in a closed-loop FNS system should be optimized without recording the original source signals from the distal nerve branches. Second, in the ankle-angle estimation stage, we estimated the ankle-angle position from the separated neural signals using DDRNN, which exhibited high estimation accuracy in terms of the similarity between the measured ankle angle and the estimated ankle angle. The proposed method could be applicable to closed-loop FNS systems to obtain robust feedback signals using only a single multichannel cuff electrode. In further work, the proposed method will be implemented in an FNS system to provide functional control of limb motions, such as slow walking and weight balancing for standing.

References

[1] T. Sinkjaer *et al.*, "Biopotentials as command and feedback signals in functional electrical stimulation systems," *Med. Eng. Phys.*, vol. 25, no. 1, pp. 29–40, Jan. 2003.

[2] P. E. Crago *et al.*, "Closed-loop control of force during electrical-stimulation of muscle," *IEEE Trans. Biomed. Eng.*, vol. 27, no. 6, pp. 306–312, Jun. 1980.

[3] W. Jensen *et al.*, "Improving signal reliability for on-line joint angle estimation from nerve cuff recordings of muscle afferents," *IEEE Trans. Neural Syst. Rehabil. Eng.*, vol. 10, no. 3, pp. 133–139, Sep. 2002.

[4] K. D. Strange and J. A. Hoffer, "Restoration of use of paralyzed limb muscles using sensory nerve signals for state control of FES-assisted walking," *IEEE Trans. Rehabil. Eng.*, vol. 7, no. 3, pp. 289–300, Sep. 1999.

[5] K. D. Strange and J. A. Hoffer, "Gait phase information provided by sensory nerve activity during walking: Applicability as state controller feedback for FES," *IEEE Trans. Biomed. Eng.*, vol. 46, no. 7, pp. 797–809, Jul. 1999.

[6] M. Haugland *et al.*, "Skin contact information in sensory nerve signals recorded by implanted cuff electrodes," *IEEE Trans. Rehabil. Eng.*, vol. 2, no. 1, pp. 18–28, Mar. 1994.

[7] M. Haugland and T. Sinkjaer, "Cutaneous whole nerve recording used for correction of food drop in hemiplegic man," *IEEE Trans. Rehab. Eng.*, vol. 3, no. 4, pp. 307–317, Dec. 1995.

[8] K. Yosida and K. Horch, "Closed-loop control of ankle position using muscle afferent feedback with functional neuromuscular stimulation," *IEEE Trans. Biomed. Eng.*, vol. 43, no. 2, pp. 167–176, Feb. 1996.

[9] T. Sinkjaer, "Integrating sensory nerve signals into neural prosthesis devices," *Neuromodulation*, vol. 3, no. 1, pp. 34–41, Jan. 2000.

[10] T. Sinkjaer *et al.*, "Biopotentials as command and feedback signals in functional electrical stimulation systems," *Med. Eng. Phys.*, vol. 25, no. 1, pp. 29–40, Jan. 2003.

[11] J. J. Struijk *et al.*, "Cuff electrodes for long-term recording of natural sensory information," *IEEE Eng. Med. Biol. Mag.*, vol. 18, no. 3, pp. 91–98, May/Jun. 1999.

[12] E. Cavallaro *et al.*, "On the intersubject generalization ability in extracting kinematic information from afferent nervous signals," *IEEE Trans. Biomed. Eng.*, vol. 50, no. 9, pp. 1063–1073, Sep. 2003.

[13] P. B. Yoo and D. M. Durand, "Selective recording of the canine hypoglossal nerve using a multicontact flat interface nerve electrode," *IEEE Trans. Biomed. Eng.*, vol. 52, no. 8, pp. 1461–1469, Aug. 2005.

[14] J. Rozman *et al.*, "Selective recording of electroneurograms from the sciatic nerve of a dog with multi-electrode spiral cuffs," *Jpn. J. Physiol.*, vol. 50, pp. 509–514, 2000.

[15] B. Wodlinger and M. Durand, "Localization and recovery of peripheral neural sources with beamforming algorithms," *IEEE Trans Neural Syst. Rehabil. Eng.*, vol. 17, no. 5, pp. 461–468, Oct. 2009.

[16] W. Tesfayesus and D. M. Durand, "Blind source separation of peripheral nerve recordings," *J. Neural Eng.*, vol. 4, no. 3, Sep. 2007, Art. no. S157.

[17] H.-S. Cheng *et al.*, "Estimation of peroneal and tibial afferent activity from a multichannel cuff placed on the sciatic nerve," *Muscle Nerve*, vol. 32, no. 5, pp. 589–599, Nov. 2005.
[18] J.-U. Chu *et al.*, "Improvement of signal-to-interference ratio and signal-to-noise ratio in nerve cuff electrode systems," *Physiol. Meas.*, vol. 33, no. 6, pp. 943–967, Jun.2012.
[19] R. R. Riso *et al.*, "Nerve cuff recordings of muscle afferent activity from tibial and peroneal nerves in rabbit during passive ankle motion," *IEEE Trans. Rehabil. Eng.*, vol. 8, no. 2, pp. 244–258, Jun. 2000.
[20] W. K. Durfee and K. E. Maclean, "Method for estimating isometric recruitment curves of electrically stimulated muscle," *IEEE Trans. Biomed. Eng.*, vol. 36, pp. 654–666, 1989.
[21] P. J. Huber, "Projection pursuit," *Ann. Statist.*, vol. 13, no. 2, pp. 435–475, Jun. 1985.
[22] A. Hyvarinen, "Fast and robust fixed-point algorithms for independent component analysis," *IEEE Trans. Neural Netw.*, vol. 10, no. 3, pp. 626–634, May 1999.
[23] M. Girolami *et al.*, "A common neural-network model for unsupervised exploratory data analysis and independent component analysis," *IEEE Trans. Neural Netw.*, vol. 9, no. 6, pp. 1495–1501, Nov. 1998.
[24] A. Hyvärinen and E. Oja, "Independent component analysis: Algorithms and applications," *Neural Netw.*, vol. 13, no. 4/5, pp. 411–430, Jun. 2000.
[25] B. Upshaw and T. Sinkjær, "Digital signal processing algorithms for the detection of afferent nerve activity recorded from cuff electrodes," *IEEE Trans. Rehabil. Eng.*, vol. 6, no. 2, pp. 172–181, Jun. 1998.
[26] A. Diedrich *et al.*, "Analysis of raw microneurographic recordings based on wavelet de-noising technique and classification algorithm: Wavelet analysis in microneurography," *IEEE Trans. Biomed. Eng.*, vol. 50, no. 1, pp. 41–50, Jan. 2003.
[27] P. E. Tikkanen, "Nonlinear wavelet and wavelet packet denoising of electrocardiogram signal," *Biol. Cybern.*, vol. 80, no. 4, pp. 259–267, Apr. 1999.
[28] W. K. Durfee and K. E. Maclean, "Methods for estimating isometric recruitment curves of electrically stimulated muscle," *IEEE Trans. Biomed. Eng.*, vol. 36, no. 7, pp. 654–667, Jul. 1989.
[29] S. Jezernik and W. M. Grill, "Optimal filtering of whole nerve signals," *J. Neurosci. Methods*, vol. 106, pp. 101–110, 2001.
[30] D. D. Suhr, "Principal component analysis vs. exploratory factor analysis," in *Proc. SUGI 30*, 2005, pp. 203–230.
[31] W. Jensen *et al.*, "Effect of initial joint position on nerve-cuff recordings of muscle afferents in rabbits," *IEEE Trans. Neural Syst. Rehabil. Eng.*, vol. 9, no. 3, pp. 265–272, Sep. 2001.
[32] P. H. Veltink *et al.*, "Nonlinear joint angle control for artificially stimulated muscle," *IEEE Trans. Biomed. Eng.*, vol. 39, no. 4, pp. 368–380, Apr. 1992.
[33] W. Jensen *et al.*, "Improving signal reliability for on-line joint angle estimation from nerve cuff recordings of muscle afferents," *IEEE Trans. Neural Syst. Rehabil. Eng.*, vol. 10, no. 3, pp. 133–139, Sep. 2002.
[34] E. Cavallaro *et al.*, "On the intersubject generalization ability in extracting kinematic information from afferent nervous signals," *IEEE Trans. Biomed. Eng.*, vol. 50, no. 9, pp. 1063–1073, Sep. 2003.

Kang-Il Song received the B.S. degree in biomedical engineering from Yonsei University, Wonju, South Korea, in 2009, and the M.S. degree in biomedical engineering from Yonsei University, Seoul, South Korea, in 2011. He is now a Ph.D. candidate at the school of electrical electronic engineering, Yonsei University, Seoul, South Korea.

Since 2008, he has been working as a Researcher at the Korea Institute of Science and Technology, Seoul, South Korea. His research interests include biomedical signal processing, pattern recognition, neuroprosthetics, rehabilitation engineering, and neuromodulation.

Jun-Uk Chu (M'05) received the B.S. degree in electrical engineering from Yeungnam University, Gyeongsan, South Korea, in 1998, and the M.S. and Ph.D. degrees in electronic engineering from Kyungpook National University, Daegu, South Korea, in 2000 and 2009, respectively.

From 2002 to 2006, he was a Researcher with the Korea Orthopedics and Rehabilitation Engineering Center, Incheon, South Korea. From 2009 to 2013, he was a Postdoctoral Fellow with the Korea Institute of Science and Technology, Seoul, South Korea. Since 2014, he has been a Senior Researcher with the Korea Institute of Machinery and Materials, Daegu, South Korea. His current research interests include neuroprosthetics, rehabilitation engineering, and pattern recognition.

Sunghee E. Park received the B.S. degree in mechanical engineering from Korea University, Seoul, South Korea, in 2015. She is currently working toward the M.S. degree at the School of Mechanical Engineering, Korea University.

Since 2010, she has been working as a Student Researcher at the Korea Institute of Science and Technology. She is now conducting a research on pathophysiology of Parkinson's disease and also on physiological responses associated with stress using animal models. Her research interests include understanding the mechanism of various neurodegenerative disorders and developing platforms where new treatments can be tested.

Dosik Hwang received the B.S. and M.S. degrees in electrical engineering from Yonsei University, Seoul, South Korea, in 1997 and 1999, respectively, and the Ph.D. degree in bioengineering from the University of Utah, Salt Lake City, UT, USA, in 2006.

From 2006 to 2008, he was a Researcher at the University of Colorado Health Science Center, Denver, CO, USA. He is currently an Associate Professor at Yonsei University, Seoul, South Korea. His research interests include biomedical signal processing, MRI, single-photon emission computed tomography, ultrasound imaging, computed-tomography reconstruction, biometrics, and computer-aided diagnosis.

Inchan Youn received the B.S. degree in biomedical engineering from In-Je University, KyungNam, South Korea, in 1996, and the M.S. degree in mechanical engineering from the University of Pittsburgh, Pittsburgh, PA, USA, in 1999, and the Ph.D. degree in biomedical engineering from Tulane University, New Orleans, LA, USA, in 2003.

From 2003 to 2006, he received Postdoc training in orthopaedics at Duke University Medical Center, Durham, NC, USA. From 2006 to 2012, he was a Senior Researcher at Biomedical Research Institute (BRI), Korea Institute of Science and Technology (KIST), Seoul, South Korea. He is currently a Principal Researcher at BRI, KIST, and a Professor at the Department of Biomedical Engineering, University of Science and Technology, Daejeon, South Korea. His research interests include the development of translational technologies in the field of biomedical instrumentation, rehabilitation and man-machine interface.